Investigation of increasing poloxamer 188 concentrations on bubble size, volumetric mass transfer, and foam generation to enable intensified bioreactor processes

Marisa Maher, Samantha Whitney, Diana Perez, Jana Mahadevan, Vivian Gasca, Sualyneth Galarza, Aayush Mehta, Amy Wood

Abstract

Intensified bioreactor processes create a need to use higher efficiency sparging systems to keep up with increased oxygen demand. High-efficiency sparger designs likely result in lower bubble size, leading to potential bubble shear impacts on mammalian cells. One strategy to achieve higher viable cell density (>100 e6 cells/mL) while managing cell shear is using increased concentrations of poloxamer (>2 g/L). In this work, the hydrodynamics within bench (3 L) and pilot scale (200 L) bioreactors were explored. Various poloxamer concentrations (2 g/L-6 g/L) and antifoam concentrations (50-500 ppm) within mock media were used to measure bubble size, volumetric mass transfer, and foam generation to understand impact and better support media additive decision making. A risk-based tool kit was created to determine sparger type and process conditions to balance bubble shear, foaming, and growth capabilities for intensified bioreactor processes. Poloxamer concentration was also explored in cell culture processes at 3 L scale, where 4 g/L was found to be ideal for growth and viability without causing toxicity to the cells. Based on these findings, 4 g/L poloxamer in media was applied to a dynamic perfusion process at bench scale demonstrating capability to support >250 e6 cells/mL at 97% viability.

Key words: poloxamer, bubble shear, bioreactor intensification, oxygen mass transfer, foam, DO% control, hydrodynamics

Introduction

In intensified bioprocessing, a higher viable cell density (VCD) is targeted to lower facility footprints and increase process productivity. To achieve a higher VCD and keep up with oxygen demand, processes are adopting the use of high-efficiency spargers within stirred-tank bioreactors to achieve increased volumetric gas transfer (k_La) targets. Achieving efficient mass transfer is possible with spargers with lower pore sizes (<50 µm) which result in smaller bubble sizes (<2 mm). Additionally, higher agitation rates can lead to increased bubble hold up time, and decreased bubble size depending on bioreactor geometry and sparger placement. However, small bubble sizes rupturing at the liquid surface, cell attachment to bubbles, and foam entrapment are causes of bubble shear with mammalian cells.[1-2] The energy from bubble burst, where smaller bubble sizes have higher energy dissipation, is estimated to be the leading cause of shear within stirred-tank bioreactors.[3] Based on one model, with a 1-2 mm bubble size, bubble shear is estimated to be magnitudes higher (10^7-10^9 W/m^3) than shear caused by agitation (10-100 W/m^3).[3] One method to protect mammalian cells from bubble shear is through surfactant additives to the media. Pluronic lowers interfacial tension of media, theorizing to lower cell damage at the liquid surface.[4] Commonly used Poloxamer 188 (P188; Pluronic F68 or PF-68) is theorized to protect and repair cell membranes.[5-6] The concentration of poloxamer in media is thought to be effective at 0.1 % (1 g/L) but shown to decrease

effectiveness with increasing cell density.[7] P188 was also found to enter mammalian cells, where overall the P188 concentration in culture medium varied by the number of cells present.[8] With variation of cell type, sparging strategy, and VCD, the optimum poloxamer concentration may need to be increased above 1 g/L for intensified processes.

Another consideration is scaling up to higher bioreactor volumes (100 - 10000 L). The height of a bioreactor poses higher risk to cell death, where the addition of poloxamer becomes more critical to reduce cell death caused by bubble shear.[1]

With the push toward process intensification and higher VCD processes, the strategy of increasing poloxamer concentration is a feasible option for enabling the use of a high-efficiency sparger with more sensitive cell lines. In one study, increasing P188 concentration to 5 g/L allowed for the use of a frit sparger to achieve 60-80 e6 cells/mL and high viability up to 200 L scale.[9] Another study found increasing P188 concentration to 5 g/L had no impact on product quality and is a feasible bubble shear mitigation strategy.[10] Additionally, this work shows a process using 4 g/L P188 enabling the use of a 50 µm microsparger and growing cell densities above 250 e6 cells/mL with high viability (97%).

To understand the effect of media additives on the process conditions in the bioreactor, a previous study explored the impact of P188 concentrations on mass transfer and bubble sizes up to 3 g/L; this study found that P188 lowers bubble size. The study also found that k_La is lowered from 0 to 0.3 g/L and begins to rise at higher concentrations (up to 3 g/L shown), depending on sparger type.[11] This work aims to explore the effect of higher P188 concentrations, up to 6 g/L, on volumetric mass transfer (k_La), bubble size, and foam generation at both 3 L and 200 L scale with mixing and several sparger types.

P188 Impurity and Cell Toxicity Considerations

There has been increased understanding around surface active compounds interacting with P188, causing molecular weight distributions and decrease in cell viability.[5,12,13] One study found that low performing lots of P188 (in terms of protecting against cell damage and supporting cell growth) had increased high molecular weight species and impurities. These lots also had increased foam stability, meaning the foam layer did not dissipate as quickly.[12] Another study found that k_La was not impacted by molecular weight distributions.[13] Lot to lot variability of source material should be considered with decision making around increasing poloxamer concentration within media.[12-,13] Throughout this work, Poloxamer 188 EMPROVE® EXPERT (SAFC, cat. no. 137097) cell culture optimized is used due to consistent molecular weight distribution and the lack of high molecular weight impurities.[14]

Materials and Methods

Mock media formulations were made with Dulbecco's Phosphate Buffered Saline (cat. no. D8537) at 1X concentration, referred to as 1X PBS, with added Poloxamer 188 EMPROVE® EXPERT cell culture optimized (SAFC, cat. no. 137097) referred to as P188. In volumetric mass transfer trials, EX-CELL® Antifoam C (cat. no. 59920C) was added at 50-100 ppm. The media used was EX-CELL® Advanced HD Perfusion Medium (cat. no. 24370C) with 4 g/L Poloxamer 188 EMPROVE® EXPERT cell culture, 50 ppm EX-CELL® Antifoam C. To evaluate k_La, two different bioreactor systems were used with dimensions described below.

	Mobius® 3 L Single-Use Bioreactor	Mobius® iFlex Bioreactor 200 L
H:D	1.8:1	2.0:1
Maximum Working Volume (L)	2.4	200
Minimum Working Volume (L)	1	40
h_{fmax}:H	0.8:1	0.8:1
h_{fmin}:h_{fmax}	2.7:1	5.0:1
d_i:D	0.55	0.38
Vessel Diameter (cm)	13.7	55.1
Impeller Geometry	Up-pumping marine (3 blades)	Down-pumping pitched blade (4 blades)
Impeller Position	On shaft, centered	Bottom mount, 15° from center
Impeller Power Number	0.3	3.6
Baffles	N/A	X - Baffle

H: bioreactor vessel height
H_{fmax}: maximum fluid height
H_{fmin}: minimum fluid height
D: bioreactor vessel diameter
d_i: impeller diameter

Table 1. Bioreactor designs evaluated for k_La

To evaluate bubble size, seven different sparger types, that belong to both 3 L and 200 L bioreactors, were evaluated with specifications described below.

Label	Name	Pore Size (µm)	Format
A	Mobius® 3 L Single-Use Bioreactor, open pipe	2300	Single drilled hole in plastic
B	Mobius® 3 L Single-Use Bioreactor, microsparger	15-30	Sintered polyethylene
C	Applikon© 3 L Glass Bioreactor, L-sparger	1000	Drilled holes in metal
D	Applikon© 3 L Glass Bioreactor, microsparger	50	Sintered Metal
E	200 L Mobius® iFlex Bioreactor, open pipe	7400	Single drilled hole in plastic
F	200 L Mobius® iFlex Bioreactor, drilled hole	150	2245 drilled holes in flexible film
G	200 L Mobius® iFlex Bioreactor, high performance	20	35433 drilled holes in flexible film

Table 2. Spargers evaluated throughout the study

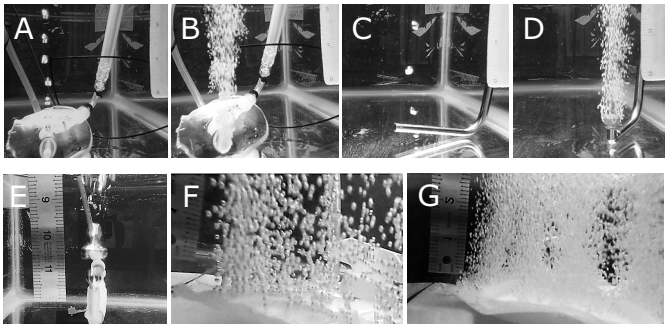

Image 1. Bubble images from spargers A-G in 1X PBS 2 g/L Poloxamer 188 EMPROVE® EXPERT, 37°C without mixing in 20 L liquid volume and near a reference measurement. Spargers A-D at 0.05 SLPM (3 L scale) and spargers E-G at 2 SLPM (200 L scale).

Bubble Size

To evaluate bubble shear risks, bubble size was measured within several mock media formulations up to 6 g/L P188 concentration. Media was imitated by using a high-salt concentration solution of 1X PBS and varying concentrations of Poloxamer 188 EMPROVE® EXPERT. A high-speed camera captured bubbles created by the sparger within the same frame as a reference measurement (a ruler). Using the software ImageJ, frames were converted into 7-10 images, and bubbles were traced in the same plane as the ruler, using it as a reference measurement within the software. 50-100 bubbles were traced per each condition and ImageJ output minimum and maximum diameter of bubbles and converted to circular bubble diameter.

Equation (Eq.) 1. $D = \sqrt{\min feret \cdot \max feret}$

Where $\min feret$=minimum bubble diameter, $\max feret$= maximum bubble diameter

Average bubble diameter (also referred to as bubble size) and standard deviations were taken for each sparger and condition. Flow rates were converted into volume of air per vessel volume (vvm) to normalize flow rate to operating rates of the sparger for further analysis.

Eq. 2. $\text{vvm} = \frac{\textit{Flow rate (SPLM)}}{\textit{Volume of reactor of originating sparger (L)}}$

a. Without Mixing

Within an acrylic tank filled to 20 L volume, spargers were obtained from respective reactors and placed near a reference measurement. Bubble size analysis was completed in the flow rate operating range of each sparger using the technique described above without mixing.

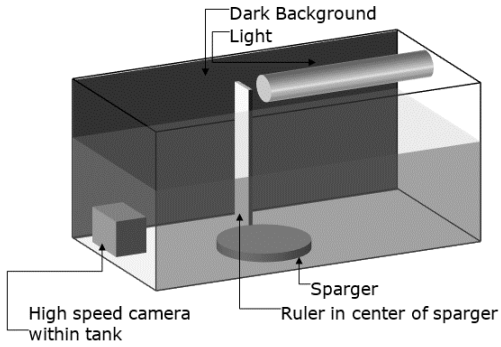

Image 2. Static bubble size evaluation set up.

Conditions	All Spargers
Volume (L)	20
Temperature (°C)	37 ± 1
Sparger	A-G from Table 2
Solutions	1X PBS 1X PBS 2 g/L P188 1X PBS 4 g/L P188 1X PBS 6 g/L P188
Power Input Per Volume (W/m³)	No mixing
Flow Rate (SLPM)	0.05, 1: spargers A-D from Table 2 2, 20: spargers E-G from Table 2

Table 3. Static bubble size test conditions

b. With Mixing, at 200 L Scale

In an acrylic tank representative of the 200 L Mobius® iFlex Bioreactor filled to 200 L volume, spargers were placed in locations consistent with the single-use bag design. A ruler was placed near the sparger and bubbles while taking the videos with a high-speed camera. Bubble size analysis was completed within the flow rate operating range of each sparger using the technique described above with no mixing, mixing at 20 W/m³, and at 100 W/m³. Agitation speeds were determined through the following equations using impeller specifications from Table 1 for each power density.

Eq. 3. $N_P = \frac{P}{\rho d^5 \omega^3}$

Where N_p= power number, P = power, ρ = density of mixing fluid d = impeller diameter, ω = angular velocity.

Eq. 4. $P_d = \frac{P}{V} = \frac{N_p \rho d^5 \omega^3}{V}$

Where V = volume, P_d= Power Density.

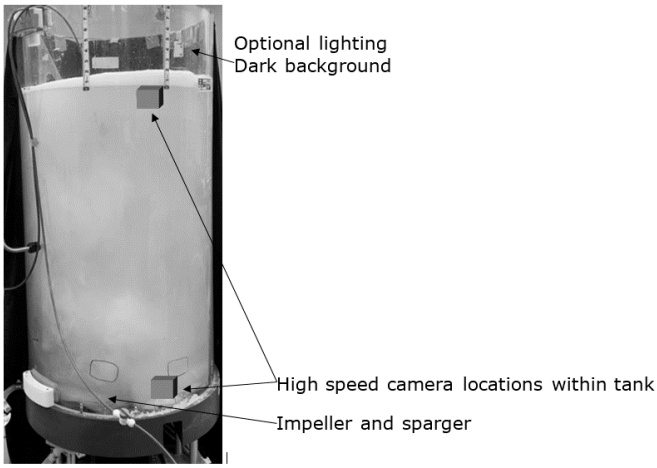

Image 3. 200 L bubble size evaluation with mixing

Conditions	200 L Scale Spargers
Volume (L)	200
Temperature (°C)	37 ± 1
Sparger	E-G from Table 2
Solution	1X PBS 4 g/L P188
Power Input Per Volume (W/m³)	No Mixing 20 100
Flow Rate (SLPM)	2 20

Table 4. 200 L bubble size evaluation with mixing

Volumetric Mass Transfer

A calibrated dissolved oxygen (DO) probe was used to measure the oxygen content of the solution. The system was purged of oxygen by sparging nitrogen until the DO reading dropped below 5%. Then, air was sparged until the system was saturated and the DO sensor reached its maximum concentration. Data from this curve was then taken in the range of 10% to 90% to calculate $k_L a$ from the following equations.

Eq. 5. $$k_L a = \frac{OTR}{C^* - C}$$

Eq. 6. $$ln\frac{(C^* - C_1)}{(C^* - C)} = k_L a * (t - t_1)$$

Where $k_L a$= volumetric mass transfer rate, OTR = oxygen transfer rate, C*= saturation concentration, C = oxygen concentration, C_1= initial gas concentration, t= time, t_1= initial time.

a. 3 L $k_L a$

A Mettler Toledo InPro® 6860i/12/120 DO sensor was calibrated with air for 100% DO. Each condition had N=2 bioreactors and N=1 repeats. This was completed with Mobius® 3 L Single-Use Bioreactor at 2 L volume.

Conditions	Mobius® 3 L Single-Use Bioreactor
Volume (L)	2
Temperature (°C)	37
Sparger	A-B from Table 2
Solutions	1X PBS 1X PBS 2 g/L P188 50 ppm Antifoam C 1X PBS 4 g/L P188 50 ppm Antifoam C 1X PBS 6 g/L P188 50 ppm Antifoam C EX-CELL® Advanced HD Perfusion Medium 4g/L P188, 50 ppm Antifoam C
Power Input Per Volume (W/m³)	20 100
Flow Rate (SLPM)	0.05 0.25 1

Table 5. Bench scale $k_L a$ conditions

b. 200 L $k_L a$

A Hamilton® VisiFerm DO Arc 120 C sensor was calibrated with air to 100% DO saturation. Each condition had N=1 bioreactors and N=3 repeats using two sensors. This was completed in the Mobius® iFlex Bioreactor 200 L.

Conditions	Mobius® iFlex Bioreactor 200 L
Volume (L)	200
Temperature (°C)	37
Sparger	E-G from Table 2
Solutions	1X PBS 1X PBS 4 g/L P188 varying 50-500 ppm Antifoam C
Power Input Per Volume (W/m³)	20 100
Flow Rate (SLPM)	2 10 20 50 (drilled hole and high performance only)

Table 6. 200 L scale $k_L a$ conditions

Foam Generation

Using the 200 L Mobius® iFlex Bioreactor at 200 L volume, foam was generated and measured at the maximum height with a tape measure from the top of the liquid height.

The foam height was collected every minute until the foam either reached the top of the tank or hit the 10-minute mark, foam rates in centimeters per minute were then calculated. For the conditions completed with antifoam, data was collected every 10 minutes for an hour each.

Image 4. 200 L foam generation evaluation

Conditions	200 L Mobius® iFlex Bioreactor
Volume (L)	200
Temperature (°C)	37
Sparger	F-G from Table 2
Solution	1X PBS 2 g/L P188 1X PBS 4 g/L P188 1X PBS 6 g/L P188 1X PBS 4 g/L P188 varying 50-350 ppm Antifoam C
Power Input Per Volume (W/m³)	20 100
Flow Rate (SLPM)	2 10 20
Power Input Per Volume (W/m³)	20 100

Table 7. 200 L scale foam generation conditions

Cell Culture

To test the impact of different P188 concentrations, a 3 L Applikon® glass bioreactor at 2 L working volume (Applikon®, Netherlands) was used for both steady state and dynamic perfusion processes using 1-4 g/L P188 and spargers C, D from Table 2.

DO (%)	pH	Sparger	Temperature (°C)	Agitation (rpm)	Media	Cell Line	Perfusion
40	6.90 ± 0.05	Sparger C with D as needed from Table 2.	37	350 until capacity 365-425	EX-CELL® Advanced HD Perfusion Medium + 1-4 g/L EMPROVE® Poloxamer 188, EX-CELL® Antifoam C added on demand	CHOZN®GS cell line producing a fusion protein	Steady state perfusion CSPR = 8 – 20 pL/cell/day Dynamic perfusion CSPR = 20-40 pL/cell/day

Table 8. Bench scale cell culture conditions to test 1-4 g/L P188 concentrations, CSPR: Cell Specific Perfusion Rate.

To optimize cell growth, A 3 L Applikon® glass bioreactor at 2 L working volume (Applikon®, Netherlands) was used for a dynamic perfusion process using 4 g/L P188 and spargers C, D from Table 2.

DO (%)	pH	Sparger	Temperature (°C)	Agitation (rpm)	Media	Cell Line	Perfusion
40	6.90 ± 0.05	Sparger C with D as needed from Table 2.	37	350 until capacity 365-425	EX-CELL® Advanced HD Perfusion Medium + 4 g/L EMPROVE® Poloxamer 188, EX-CELL® Antifoam C added on demand	CHOZN®GS cell line producing a fusion protein	Dynamic perfusion CSPR = 40 pL/cell/day

Table 9. Bench scale cell culture conditions to optimize cell growth.

Results

Bubble Size

a. Without Mixing

The addition of P188 is reported to decrease surface tension of liquids, and lower bubble size. Surfactant molecules are formed above the critical micelle concentration (~0.3 g/L for P188). This creates a film around the bubble, thus creating rounder bubbles and easier detachment from sparger surface.[11]

In the data collected, bubble size decreased when increasing concentration from 0-2 g/L P188, and stayed relatively steady >2 g/L P188 (Fig. 1). From 0-2 g/L P188, the bubble size of the 3 L Mobius® microsparger (15-30 µm), Mobius® iFlex 200 L high performance (20 µm), Applikon© microsparger (50 µm), 200 L Mobius® iFlex drilled hole (150 µm), Applikon© L- sparger (1000 µm), Mobius® open pipe (2300 µm) decreased by 62%, 25%, 29%, 12%, 45%, 44%, by averaging flow rates data, respectively. The 200 L Mobius® iFlex open pipe (7400 µm) increased by 2%, within standard deviation of 0 g/L bubble size, by averaging flow rates data. Bubble size changes with P188 concentration are highly dependent on sparger design, where irregular pore sizes may have more of a change in size and shape than uniform pore sizes.[11] Pore size was also correlated to bubble size within each P188 concentration solution in 1X PBS. The pore size of the sparger correlates to the bubble size linearly in the full range of pore sizes tested, 20 to 7400 µm; however it was observed that in the lower range of pore sizes tested, 20-2300 µm, the

pore size to bubble size relationships are best modelled by the power function (Fig. 2).

With lower bubble size at higher P188 concentrations (>2 g/L), the gas hold-up and surface area are increased.[11] This can be observed with the evaluation of flow rate on bubble size with the addition of P188. Without P188, the flow rate impacts bubble size exiting the surface of the sparger. At higher operating flow rates, bubbles are seen to be expanded at the surface of open pipe spargers with larger pore sizes (>1000 µm) (Fig. 3). With the addition of P188, surface tension is lowered, and bubble sizes are less impacted by flow rate (Fig. 4).

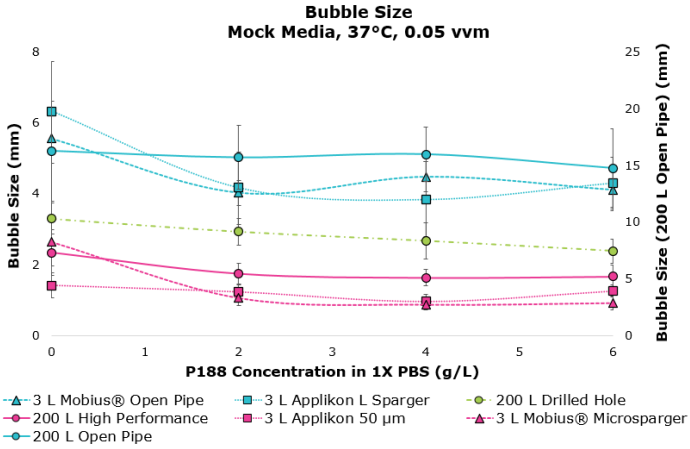

Figure 1. Bubble size measured up to 6 g/L of P188 at 0.05 vvm of sparger scale and 37°C. In all sparger types, bubble size was lowered or within standard deviation at 0-2 g/L P188 and remained relatively steady above 2 g/L. Error bars are standard deviations. Secondary Y-Axis is for the 200 L Open Pipe data all other data sets are displayed on the primary Y-axis.

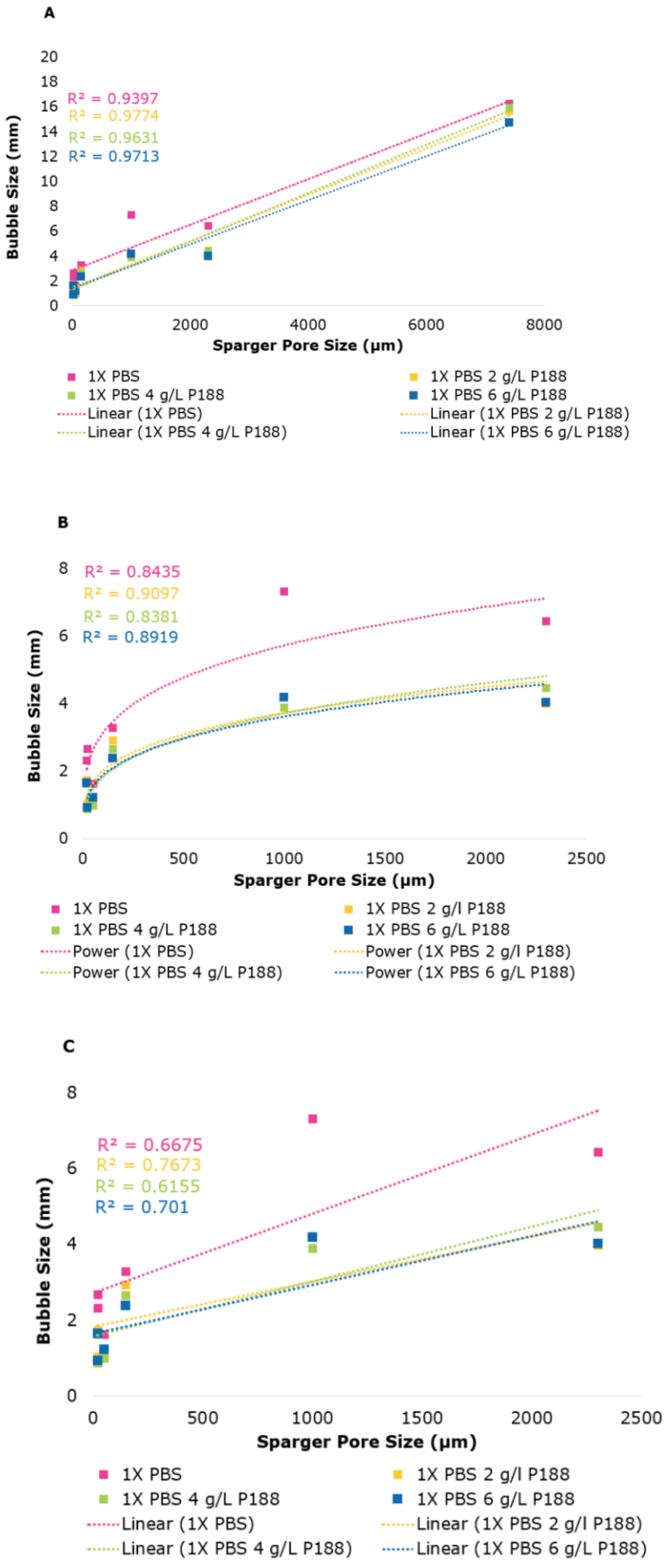

Figure 2. Bubble size correlated with pore size of sparger from 0-6 g/L solutions in 1X PBS, at 37°C and 0.05 vvm. A. with up to 7400 µm pore size showing a linear relationship, B. up to 2300 µm pore size with a power relationship, and C. up to 2300 µm pore size with a linear relationship showing lower correlation than B.

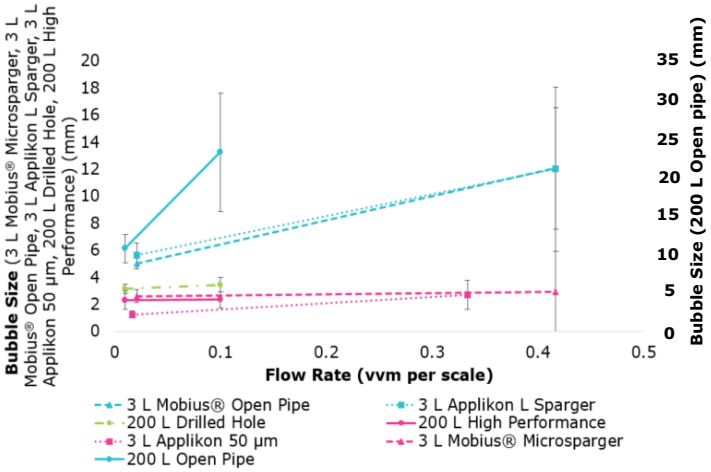

Figure 3. Impact of flow rate on bubble size in 1X PBS without poloxamer at 37°C. In open pipe spargers with larger pore sizes (>1000 µm), increasing flow rate results in increased bubble size, with high variation. In smaller pore sized spargers (<100 µm), flow rate effect on bubble size is minimal. Error bars are standard deviations.

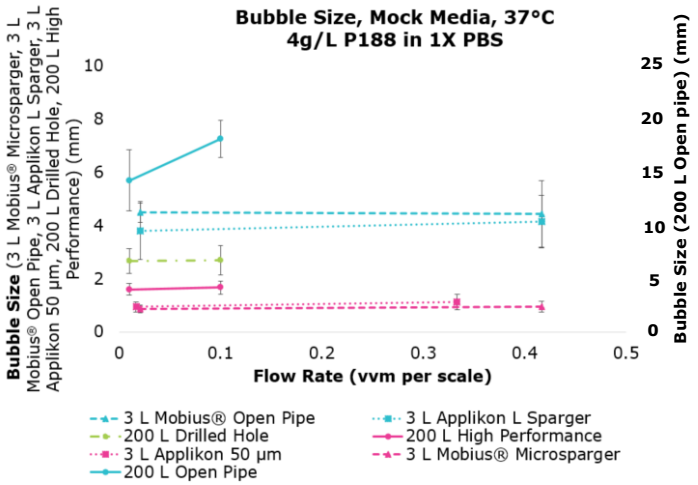

Figure 4. Impact of flow rate on bubble size in 1X PBS with 4 g/L P188 at 37°C. With the addition of P188, the impact of flow rate is minimal, besides the open pipe sparger with the largest pore size (7400 µm). Error bars are standard deviations.

b. With Mixing, at 200 L Scale

Bubble size was compared across two vessels at 20 L scale and 200 L scale. Under the same conditions, the bubble size is compared to understand the impact of the vessel change to 200 L with agitation abilities. At the exit of the sparger, there was a slight impact of the hydrostatic pressure on the open pipe sparger, matching literature.[15] The comparison between the bubble size analysis at 20 L scale test bed and 200 L scale bioreactor prototype was verified (Fig. 5).

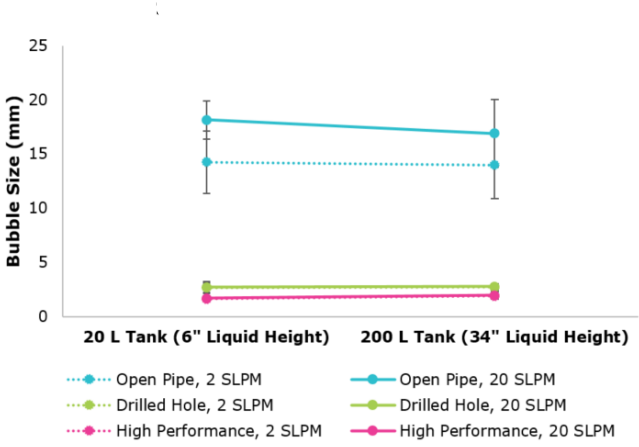

Figure 5. Comparison of bubble size at exit of sparger, between 20 L & 200 L tanks, in 1X PBS, 4 g/L P188 at 37°C with no mixing. Impact of hydrostatic pressure at the exit of the sparger seen within open pipe sparger, where more liquid height resulted in a slightly lower bubble size. Minimal effect seen for drilled hole and high performance spargers, within standard deviation. Error bars are standard deviations.

Bubble size was evaluated at locations near the exit of the sparger and near the liquid surface to understand the hydrodynamic effects with and without mixing in the presence of 4 g/L P188.

At the top of the tank, for the open pipe (7400 µm) sparger, the bubble size was decreased as the power density increased (Fig. 6). Visually, the large bubbles were broken up as they travelled to the top of the tank, especially at higher power per volume input. For the drilled hole (150 µm) and high performance (20 µm) spargers, the bubble diameters increased as they travelled to the top of the tank with and without mixing, likely caused by the decrease of hydrostatic pressure (Fig. 7, Fig. 8).[15] No clear trends were observed with the interaction between flow rate and power on bubble diameter within this solution (1X PBS 4g/L P188). With the onset of power density from 0-20 W/m^3 (20 W/m^3 has a Reynolds Number (Re) of 16,200 in this bioreactor) bubble size is reported to decrease at the sparger exit by 8% for open pipe, 19% for drilled hole, and 12% for high performance by averaging the flow rate data. From 20-100 W/m^3 (up to Re of 114,000) bubble size is estimated to decrease 13% for the open pipe sparger, and no decrease is observed for drilled hole and high performance spargers, within standard deviation. Similar trends are seen at the top of the tank. In this configuration, the drilled hole and high performance spargers are located on the bottom of the tank, close to the impeller. This suggests that, with the onset of more turbulent mixing conditions, the down-pumping motion increases bubble residence time and bubble movement within the tank, lowering bubble size.[16]

Both drilled hole and high performance spargers, with smaller pore sizes, reached a plateau in bubble size at 20 W/m^3, although it was visually observed that bubbles remained longer in the tank at 100 W/m^3.

k_La increased from 20-100 W/m^3, showing bubble hold up is likely the cause of higher volumetric mass transfer rather than changes in bubble size when increasing power density. For the open pipe sparger, increased power density at 20-100 W/m^3 continued to break up the bubbles, likely due to the larger overall bubble size.

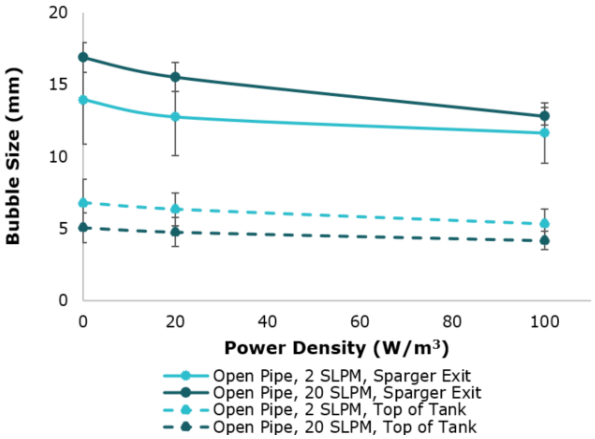

Figure 6. Impact of power density on bubble size for open pipe sparger (7400 µm single drilled hole) at 37°C in 1X PBS, 4 g/L P188. Bubble size is decreases with the onset of mixing at both 2 and 20 SLPM. Bubbles were visually appeard to break up as they travelled from the exit of the sparger to the top of the tank. No clear trend observed with flow rate. Error bars are standard deviations.

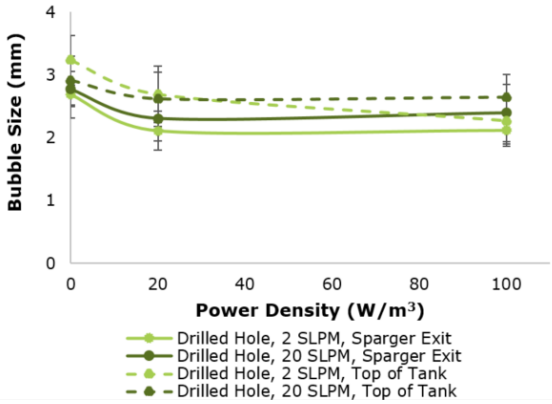

Figure 7. Impact of power density on bubble size for the drilled hole sparger (150 µm drilled holes in film) at 37°C in 1X PBS, 4 g/L P188. Bubble size decreases with the onset of mixing at both 2 and 20 SLPM. Bubbles were seen to expand from the exit of the sparger to the top of the tank. Higher flow rate yielded slightly larger bubble size. Error bars are standard deviations.

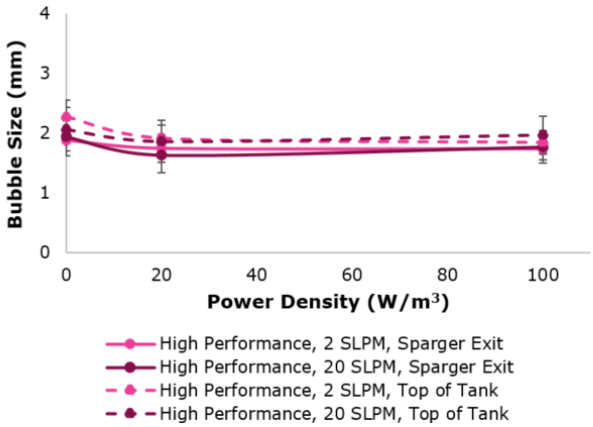

Figure 8. Impact of power density on bubble size for the high performance sparger (20 µm drilled holes in film) at 37°C in 1X PBS, 4 g/L P188. Bubble size decreases with the onset of mixing at both 2 and 20 SLPM. Bubbles were seen to expand from the exit of the sparger to the top of the tank. No clear trend of flow rate. Error bars are standard deviations.

Volumetric Mass Transfer

k_La was measured in 1X PBS from 0 - 6 g/L P188 to understand the impact of increasing concentration on mass transfer performance. In all solutions, k_La was a function of power input and gas flow rate, and likely gas hold up, matching literature.[17-18] From 0-2 g/L P188, the full formation of the micelle layer on the bubble is thought to be formed.[11]

Here, the diffusion through the surfactant layer is thought to be the rate limiting step, dominated by the bubble size.[11] For another study, in lower concentrations (<0.3 g/L), k_La was shown to decrease, yet at higher P188 concentrations, the k_La is increased for sintered spargers, and remained steady for ring spargers.[11]

a. 3 L k_La

In the data collected, k_La decreased from 0-2 g/L for the open pipe (2300 µm; Fig.9) while it increased for the microsparger (15-30 µm; Fig. 10), showing correlation to literature theories. Increasing poloxamer concentrations from 2 to 6 g/L did not result in consistently increasing or decreasing trends for neither the open pipe sparger nor the microsparger at the three flowrates tested. There is a strong dependence on sparger type and bubble size with the impact of P188 addition on k_La expected in the bioreactor.

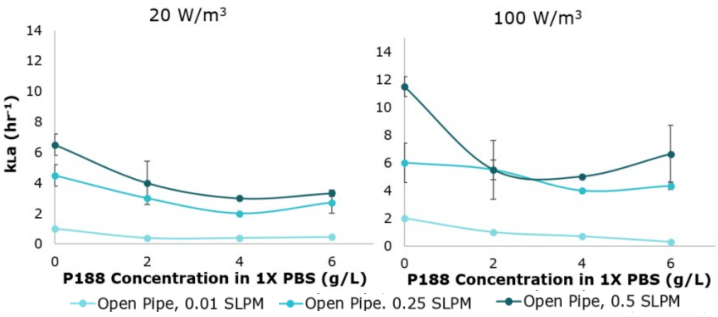

Figure 9. Impact of P188 concentration in 1X PBS on k_La using a 3 L Mobius® open pipe sparger (2300 µm) 37°C in 2 L working volume. With increasing P188 concentration from 0 – 2 g/L, k_La is decreased or within standard deviation of 0 g/L. Higher flow rate and power density results in higher k_La at each solution. All solutions with P188 have 50-100 ppm EX-CELL® Antifoam C. Error bars are standard deviations.

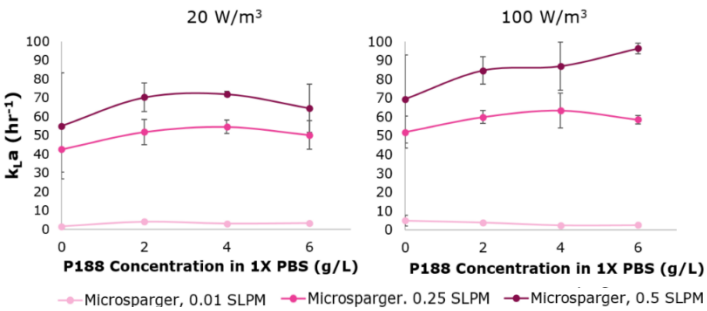

Figure 10. Impact of P188 concentration in 1X PBS on k_La using a 3 L Mobius® microsparger (15-30 µm) at 37°C in 2 L working volume. With increasing P188 concentrations from 0 – 2 g/L, k_La is increased or within standard deviation of 0 g/L P188 Higher flow rate and power density results in higher k_La at each solution. All solutions with P188 have 50-100 ppm EX-CELL® Antifoam C. Error bars are standard deviations.

In addition, the k_La in mock media formulations with and without P188 were compared to a media containing 4g/L P188 to understand the mass transfer performance differences. This enables accurate estimation of maximum VCD capabilities of the system based on sparge rates, % oxygen in gas feed, power per volume input, and k_La characterization without cells. The maximum VCD of the system can then be estimated with the following mass balance:

Eq. 7. $OTR = OUR = kLa\ (C^* - C) = qO_2 * VCD$

Where OUR= oxygen uptake rate, qO_2= cell specific oxygen uptake rate.

When comparing mock media formulations to media, there were again different trends in mass transfer based on bubble size and sparger type. For the open pipe sparger, the 1X PBS 4 g/L P188 solution was most similar to media across 3 flow rates and 2 power values. The addition of P188 seemed to have a mass transfer inhibiting effect at this bubble size (Fig. 11). For the microsparger, the media behaved most similarly to 1X PBS without media additive, where in this sparger type, the addition of P188 seemed to improve mass transfer (Fig. 12). This suggests that the media may inhibit mass transfer performance through other additives. Comparison from mock media to media is best estimated through different combinations of mock medias per sparger type.

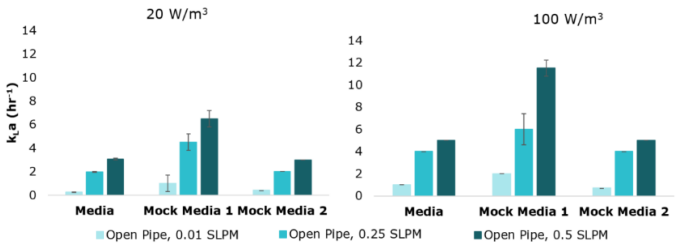

Figure 11. Comparison of cell culture media to mock medias on 3 L Mobius® Open Pipe (2300 µm) at 37°C in 2 L working volume. Cell culture media is EX-CELL® Advanced HD Perfusion Medium with 4g/L Poloxamer 188 EMPROVE® EXPERT cell culture and 50 ppm EX-CELL® Antifoam C. Mock Media 1 is 1X PBS and Mock Media 2 is 1X PBS 4g/L P188. For the open pipe sparger, Mock Media 2 is seen to be more representative of media for flow rates and powers tested. Error bars are standard deviations.

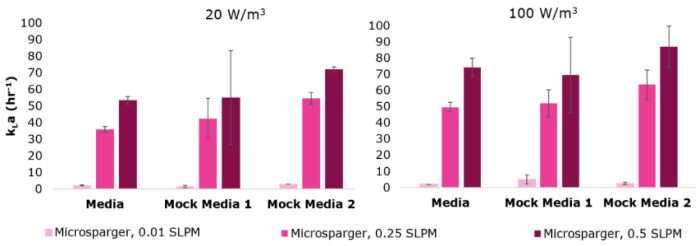

Figure 12. Comparison of cell culture media to mock medias on 3 L Mobius® microsparger (15-30 µm) at 37°C in 2 L working volume. Cell culture media is EX-CELL® Advanced HD Perfusion Medium with 4g/L Poloxamer 188 EMPROVE® EXPERT cell culture and 50 ppm EX-CELL® Antifoam C, Mock Media 1 is 1X PBS and Mock Media 2 is 1X PBS 4g/L P188. For the Microsparger, Mock Media 1 is seen to be more representative of media for flow rates and powers tested. Error bars are standard deviations.

b. 200 L k_La

At the 200 L scale, k_La was measured using a buffer of 1X PBS with 4 g/L Poloxamer 188 EMPROVE® EXPERT and 50 ppm EX-CELL® Antifoam C for the open pipe (7400 µm), drilled hole (150 µm) and high performance (20 µm) spargers. Here similar trends were observed to those found in the bench scale studies. There is a strong dependency on sparger type and bubble size which impact the effects in mass transfer performance with P188 additives. For the open pipe and drilled hole spargers, the k_La was within standard deviation of 0 g/L or decreased from 0 – 4 g/L P188, showing some inhibition on mass transfer at this threshold of bubble sizes (Fig. 13, Fig. 14). For the high performance sparger, k_La increased with the addition of P188 additives from 0 – 4 g/L (Fig. 15).

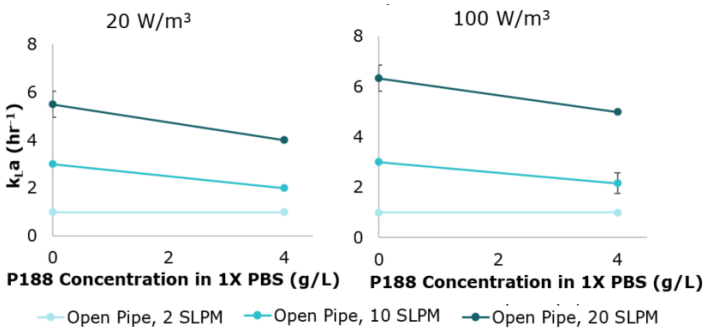

Figure 13. Impact of P188 concentration in 1X PBS on k_La using an open pipe sparger (7400 µm) at 37°C in 200 L working volume. With increasing P188 concentrations from 0-4 g/L, KLa tends to decrease, though the effect is minimized and unapparent at the lowest flow rate. Higher flow rate results in higher kLa in each solution. Higher power density results in a similar or slightly increased kLa, an effect most apparent in the highest flow rate condition. Error bars are standard deviations.All solutions with P188 have 50-100 ppm EX-CELL® Antifoam C.

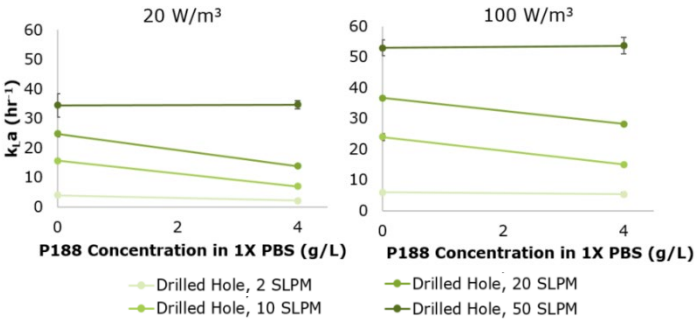

Figure 14. Impact of P188 concentration in 1X PBS on k_La using a drilled hole sparger (150 µm) at 37°C in 200 L working volume. With increasing P188 concentrations, kLa decreases for the mid and low flow rate range and remains similar at the highest flow rate. Higher flow rate and power density results in higher kLa for each solution. Error bars are standard deviations.

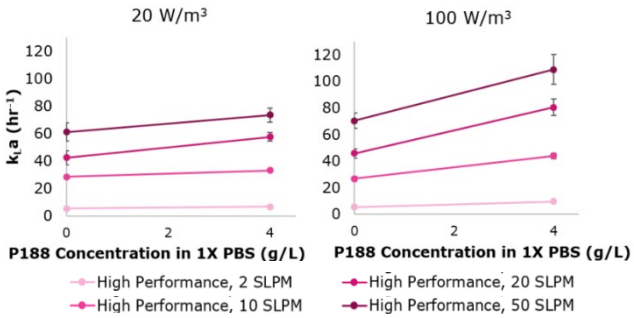

Figure 15. Impact of P188 concentration in 1X PBS on k_La using a high performance sparger (20 µm) at 37°C in 200 L working volume. With increasing P188 concentrations from 0 – 4 g/L, k_La is generally increased. Higher flow rate and power density results in higher k_La at each solution. Error bars are standard deviations. All solutions with P188 have 50-100 ppm EX-CELL® Antifoam C.

Furthermore, the addition of Antifoam C was evaluated. At 20 SLPM and 20 W/m³, k_La was measured N=3, and Antifoam C concentrations were spiked in from 50-500 ppm before immediately repeating the k_La trials. Results showed little dependence of antifoam at 50-500 ppm to mass transfer (Fig. 16). A previous study found the addition of antifoam reduces k_La performance from 0% antifoam in solution, however, the studies were performed at concentrations of <50 ppm.[19]

Another study stated antifoam only decreases k_La in low antifoam concentrations, based on antifoam type. Above the critical concentration of the specific antifoam, antifoam begins to improve k_La.[20] It was also shown that antifoam had little effect on bubble size (specific area, a), and more impact on film coefficient, k_L.[20] The critical concentration was not found as part of this study for Antifoam C. In intensified processes, especially at higher flow rates, the use of antifoam will likely be needed above 50 ppm, where these studies indicated that effects of adding 50 – 500 ppm on k_La would be minimal. Although k_La was not seen to be impacted by antifoam from 50-500 ppm within this study, it is unknown if there are other interactions with the media components, perfusion filtration, sensors, or cells that could further decrease mass transfer effects from antifoam addition or impact the overall process performance.

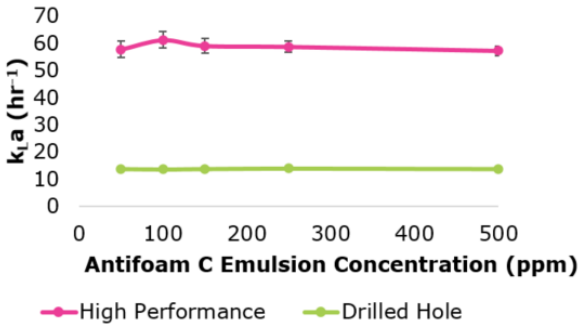

Figure 16. Impact of Antifoam C Emulsion concentration from 50-500 ppm in 1X PBS 4 g/L P188 at 20 SLPM, 37°C and 20 W/m³ on k_La where minimal impact is shown under these conditions.

Foam Generation

Foam generation was characterized by varying flow rate, poloxamer concentration, power density, and sparger type, in a design of experiments (DOE) format. The biggest contributing factors to foam generation were flow rate and sparger type (Fig. 17). For the drilled hole sparger (150 µm), flow rate was the highest contributor to foaming. Higher power density also led to increased foam generation at all flow rates. For the high performance sparger (20 µm), flow rate also had the largest effect on foam generation. The increase of P188 concentration had minimal impact on foaming with both sparger types.

At 10-20 SLPM for both sparger types, the foaming rates are too high for realistic cell culture operation without antifoam in the bioreactor. Cell culture conditions such as media type, perfusion strategy, and antifoam concentration will likely impact foaming rates; although this study gives an indication of general risk profiles associated with process conditions.

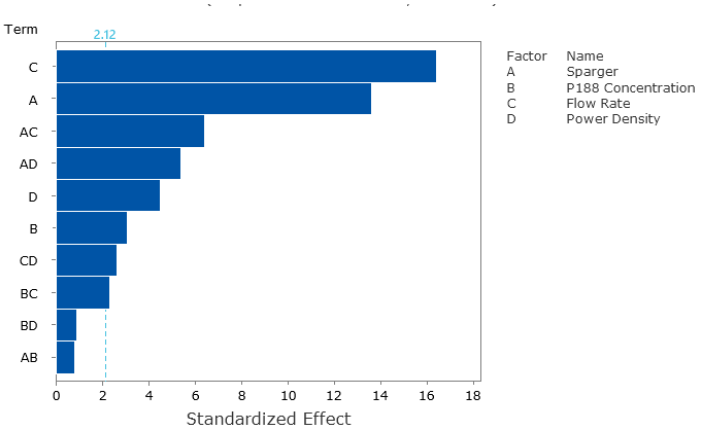

Figure 17. Pareto chart of standardized effects of each factor in foam generation DOE (response is foam rate, α = 0.05). Flow rate is the highest contributor.

Flow Rate (SLPM)	Poloxamer (g/L)	Power Density (W/m³)	Foam Rate (cm/min)	
			High Performance (HP)	Drilled Hole (DH)
2	2	20	1.00	0.30
		100	0.60	0.30
	4	20	0.65	0.20
		100	0.65	0.30
	6	20	0.70	0.20
		100	0.80	0.35
10	2	20	4.18	0.75
		100	4.18	2.56
	4	20	4.67	1.10
		100	4.67	3.42
	6	20	5.00	0.95
		100	4.60	2.44
20	2	20	8.80	5.25
		100	8.40	6.57
	4	20	9.60	6.29
		100	9.60	9.00
	6	20	9.40	5.88
		100	9.40	8.00

Table 10. Foam generation with varying flow rate, poloxamer concentration (2, 4, 6 g/L) in 1X PBS, and power density in Mobius® iFlex Bioreactor at 200 L volume. Conditional formatting shows foam generation risks at process conditions, where darker color indicates more risk to the process.

Risk Analysis and Control

Results of k_La, bubble size, estimated supported VCD, and foam generation (Table 10), are mapped and summarized as a risk-based tool to guide the selection of sparger type and process conditions (flow rate, power density) with an initial P188 concentration of 4 g/L at the 200 L scale Mobius® iFlex Bioreactor (Table 11). For example, to reach >100 e6 cells/mL, either the high performance (HP) sparger or drilled hole (DH) sparger can be used. With the HP sparger, flow rates of 10 SLPM would be required. With the DH sparger, flow rates of 20 SLPM would be required. Since flow rate is the highest contributor towards foam, the use of the HP sparger is estimated to reduce flow rate and foam levels while supporting higher VCD. The caveat being a lower bubble size required (higher bubble shear risk). Increasing power density would have little impact on VCD capacity for the HP sparger, but would greatly improve the VCD capacity for the DH sparger.

Flow Rate (SLPM)	Poloxamer 188 (g/L)	Power Density (W/m³)	Estimated VCD (e6 cells/ mL) in Media with 4g/L P188*		4 g/L Foam rates (cm/min)		Average Bubble Size at top of tank (mm), 200 L volume**	
			HP	DH	HP	DH	HP	DH
2	4	20	24	9	0.65	0.20	1.9	2.7
		100	24	23	0.65	0.30	1.8	2.3
10		20	123	30	4.67	1.10	1.9	2.7
		100	116	65	4.67	3.42	1.9	2.4
20		20	184	60	9.60	6.29	1.9	2.6
		100	198	122	9.60	9.00	2	2.6

Table 11. Risk summary with varying power density, flow rate, and poloxamer concentration in 1X PBS on bubble size, k_La, foam, and correlation to estimated supported VCD in media with 4 g/L P188 at 200 L scale with drilled hole (DH) and high performance (HP) spargers. Conditional formatting indicates risk level for each parameter, where darker color indicates higher risk to the process.

*VCD is estimated from kLa using Eq. 7 from most representative mock media to media from bench scale studies (1X PBS for HP, 1X PBS 4g/L P188 for DH) using a qO2 of a moderately consuming CHO cell line, 5 pmol O2/cell/day.
** 10 SLPM condition is interpolated

To further evaluate process control in an intensified bioreactor for foam generation, different EX-CELL® Antifoam concentration effects on foam rate were evaluated by varying sparger type and power density. This study was completed with a flow rate of 20 SLPM because of its high foam accumulation previously seen in the foam generation DOE. The results of this study showed the significant effect antifoam can have on the foam rate. However, other factors, such as media type, may have different effects on the foam rate and different amounts of antifoam may be needed to manage each unique process.

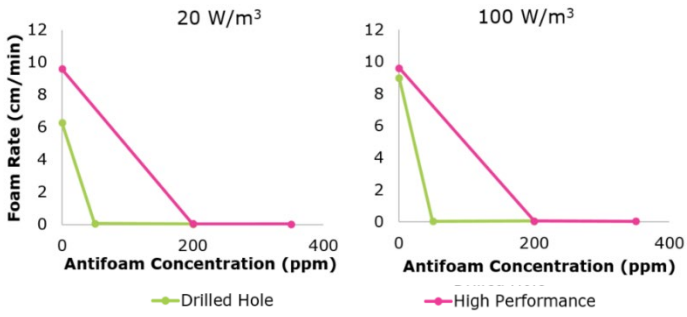

Figure 18. Foam rate with the immediate addition of antifoam. Foam rate is reduced for both the drilled hole and high performance spargers at 20 SLPM.

Cell Culture

To optimize cell growth using the CHOZN®GS cell line producing a fusion protein, the ideal level of P188 concentration was explored. Through baffled flask experiments, it was found there was little impact on cell growth from 1 to 5 g/L P188 between 0-1% Antifoam C (AF). Cell growth inhibition was seen at 10 g/L P188 between 0 - 0.5% AF. At 1% AF cell growth was not negatively impacted with 10 g/L P188. Above 1% AF and 10 g/L P188, further growth inhibition was seen (Fig. 19). From the baffled flask experiments, the process performance was explored under 5 g/L due to potential cell toxicity at 10 g/L. In a 3 L bioreactor, 1 g/L and 4 g/L P188 was compared to see the effects of increasing concentration as a means to increase shear protectivity and enable high VCD. Here, 4 g/L P188 increased VCD capabilities for both dynamic and steady state perfusion processes where the 1 g/L P188 viability dropped after reaching a VCD of 100 e6 cells/mL due to lack of shear protectant. The 4 g/L P188 reached higher cell densities compared to the 1 g/L conditions, and led to lower perfusion rate and higher cell specific productivity (Fig. 20, Table 12).

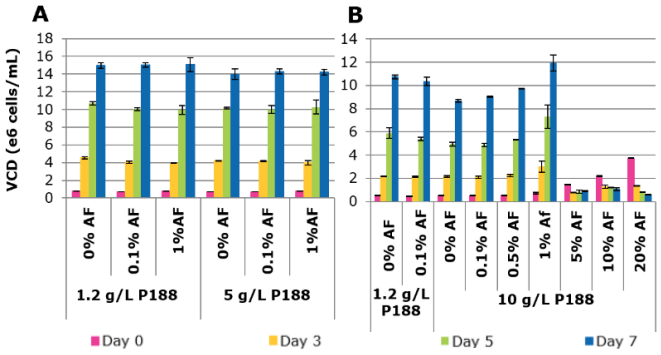

Figure 19. Baffled flask experiments using the CHOZN®GS cell line producing a fusion protein comparing cell growth at 1.2 g/L P188 to 5 g/L (A), and 1.2 g/L to 10 g/L (B) at various levels of antifoam.

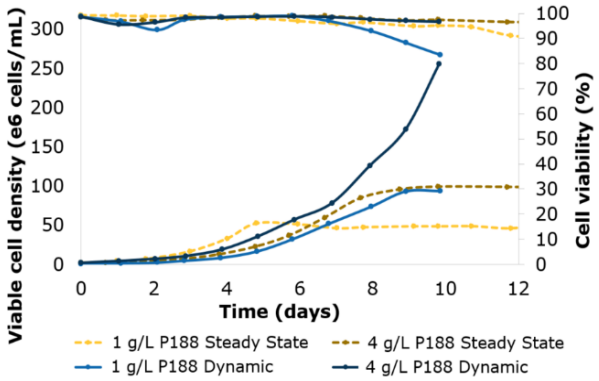

Figure 20. Comparison of 1 g/L and 4 g/L P188 on steady state and dynamic cell culture processes. A concentration of 4 g/L led to higher cell density and cell viability.

	P188 (g/L)	Perfusion Rate (vvd)	CSPRmin (pL/cell/day)	q_P (pg/cell/day)
Steady State	1	~2	~40	8
	4	~2	~20	15
Dynamic	1	~2	~20	11
	4	~2	~8	18

Table 12. Comparison of 1 g/L and 4 g/L P188 on steady state and dynamic cell culture processes. A concentration of 4 g/L P188 led to lower CSPR and higher cell-specific productivity (q_P).

The addition of 4 g/L P188 allowed the use of Applikon© 50 µm microsparger (sparger D in Table 2 characterized throughout the study) in dynamic perfusion. This kept up with oxygen demand without reducing cell viability for CHOZN® GS cell line producing a fusion protein in EX-CELL® Advanced HD Perfusion Medium + 4 g/L P188. Sparging strategy did not appear to impact cell health during the process.

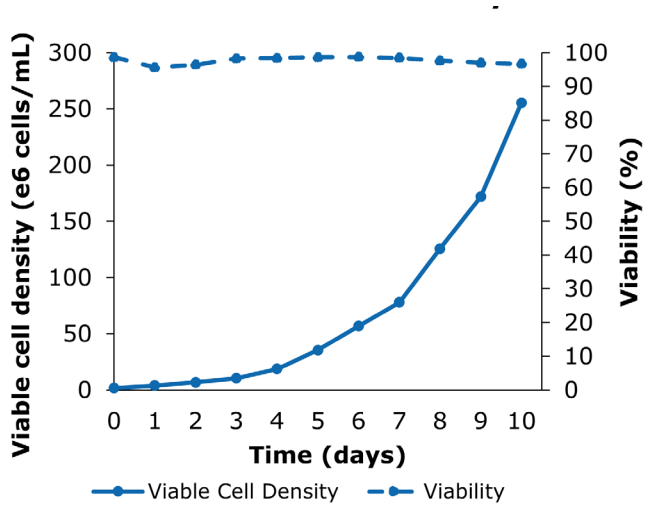

Figure 21. Cell growth and viability for perfusion cell culture. Strategy reached >250 e6 cells/mL at 97% viability.

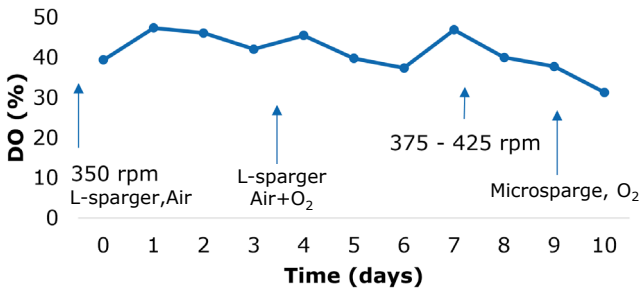

Figure 22. DO control strategy using spargers C and D from Table 2 maintained 40% DO.

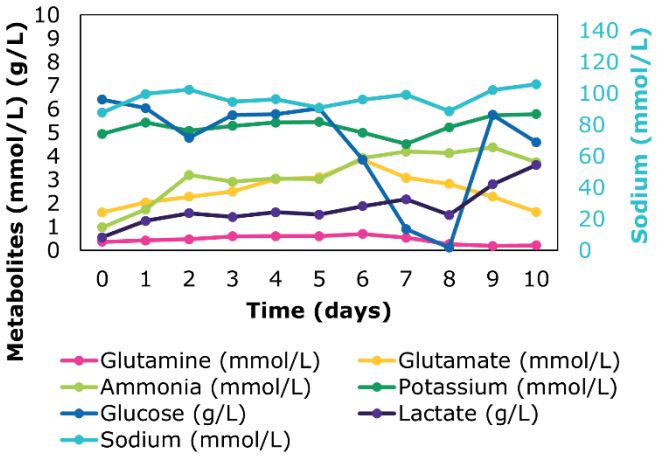

Figure 23. Metabolite profiles during cell culture process exploring DO control strategies. No clear trends indicating cell health issues from increasing agitation from 350 to 425 rpm nor from switching from L-sparger to microsparger are observed.

Conclusion and Discussion

Hydrodynamics (Bubble size, k_La, Foam Generation)

This study characterized stirred tank bioreactor gassing hydrodynamics at both 3 L and 200 L scale and was able to provide insights into practical trends and effects of varying P188 concentrations up to 6 g/L.

Bubble size was decreased from 0-2 g/L P188, matching literature.[11] Above 2 g/L, the bubble size was observed to stay constant. The increase in P188 concentration seemed to dampen the impact of bubble size changes due to flow rate, likely caused by the decrease in surface tension near the sparger. At 200 L scale with mixing, the onset of agitation lowered bubble size. Bubble size was observed to grow from the sparger exit to the top of the tank for both drilled hole spargers (150 µm) and high performance spargers (20 µm) and conversely was observed to be broken up as they travelled to the liquid surface for the open pipe sparger (7400 µm).

Trends for k_La were consistent across bench scale and pilot scale reactors. Sparger type and pore size affected the k_La trends as a result of changing P188 concentration. Smaller pore size (<50 µm) spargers resulted in a trend towards increasing k_La with added P188 concentration from 0 to 2-6 g/L. In literature, for microspargers/small pore sizes, an initial decrease in k_La at the critical micelle concentration (0.3 g/L) was observed, followed by an increase in k_La at concentrations above this threshold, therefore matching the trends observed in this study.[12] For open pipe and drilled hole spargers with larger pore sizes (>150 µm) the addition of P188 from 0 to 2-6 g/L resulted in a general trend towards lower k_La. k_La values in mock medias with and without P188 and Antifoam C were also compared to EX-CELL® Advanced HD Perfusion Medium + 4g/L EMPROVE® Poloxamer 188 EX-CELL® + 50 ppm Antifoam C at bench scale in the Mobius® microsparger (15-30 µm) and Mobius® open pipe (2300 µm). This showed mock media without P188 gave similar k_La values to EX-CELL® Advanced HD Perfusion Medium for the microsparger (<2 mm bubble size) and mock media with P188 gave most similar k_La values to EX-CELL® Advanced HD Perfusion Medium for the open pipe sparger (>2 mm bubble size). Because these trends are driven by bubble size, it is theorized that similar results can be expected within the 200 L scale system, where the k_La value most representative to the EX-CELL® Advanced HD Perfusion Medium for the drilled hole sparger would be drawn from values derived in the mock media solution that includes P188, where for the high performance sparger the most representative k_La value would be drawn from the studies using mock media without P188.

This allows for a more accurate estimation of the expected VCD capabilities at pilot scale per across flow rates, agitation rates, and sparger type.

A DOE to characterize foam generation was completed at 2 g/L P188 and 6 g/L P188 in 1X PBS with the factors of sparger type (high performance, drilled hole), flow rate, and power density. The main contributing factor to foam generation was flow rate. The drilled hole sparger was found to be impacted by P188 concentration, flow rate, as well as power density, where higher power density and P188 concentration led to increased foam generation. For the high performance sparger, higher foam rates were seen comparatively. Again, flow rate had the highest impact on foam generation, where P188 concentration and power density had lower impact, likely caused by the lower bubble sizes in the system. In all cases, the use of antifoam is recommended to control foam levels in an intensified bioreactor process.

Lastly, data for k_La, VCD estimations, and foam generation were combined for a risk-based tool. A viable strategy to improving intensified process control would be to choose P188 concentration in media from trends seen in this study, along with cell screening studies. Then, the risk-based tool could be used to choose process conditions and sparger type to balance shear, foaming, and VCD capacity considerations.

Increased P188 Concentration on Cell Culture Performance

With the rise of intensified processes, the strategy of increasing P188 concentration (up to 5 g/L) has shown success in improving growth, viability, and titer in higher cell density processes (>60 e6 cells/mL).[9] In this study, raising the P188 concentration to 4 g/L allowed for successful use of an Applikon© 50 µm microsparger, reaching >250 e6 cells/mL at 97% viability with dynamic perfusion. This demonstrates a successful implementation of this strategy.

Optimized P188 concentrations are highly dependent on cell line, cell density targets, sparger type, and cell specific oxygen uptake rates. Nevertheless, there is promise with P188 concentration as a factor to reduce bubble shear with the use of a high-efficiency sparger with increased oxygen demands within intensified processes. This work provides increased understanding of gassing hydrodynamics within typical stirred tank bioreactor systems based on balancing oxygenation performance and shear.

References

1. Meier, Steven J., T. Alan Hatton, and Daniel IC Wang. "Cell death from bursting bubbles: role of cell attachment to rising bubbles in sparged reactors." Biotechnology and bioengineering 62.4 (1999): 468-478.

2. Chisti, Yusuf. "Animal-cell damage in sparged bioreactors." Trends in biotechnology 18.10 (2000): 420-432.

3. Garcia-Briones, Miguel A., Robert S. Brodkey, and Jeffrey J. Chalmers. "Computer simulations of the rupture of a gas bubble at a gas—liquid interface and its implications in animal cell damage." Chemical engineering science 49.14 (1994): 2301-2320.

4. Hu, Weiwei, Claudia Berdugo, and Jeffrey J. Chalmers. "The potential of hydrodynamic damage to animal cells of industrial relevance: current understanding." Cytotechnology 63 (2011): 445-460.

5. Chang, David, et al. "Investigation of interfacial properties of pure and mixed poloxamers for surfactant-mediated shear protection of mammalian cells." Colloids and Surfaces B: Biointerfaces 156 (2017): 358-365.

6. G Moloughney, Joseph, and Noah Weisleder. "Poloxamer 188 (p188) as a membrane resealing reagent in biomedical applications." Recent patents on biotechnology 6.3 (2012): 200-211.

7. Chalmers, Jeffrey J. "Mixing, aeration and cell damage, 30+ years later: what we learned, how it affected the cell culture industry and what we would like to know more about." Current Opinion in Chemical Engineering 10 (2015): 94-102.

8. Gigout, Anne, Michael D. Buschmann, and Mario Jolicoeur. "The fate of Pluronic F-68 in chondrocytes and CHO cells." Biotechnology and bioengineering 100.5 (2008): 975-987.

9. Xu, Sen, et al. "Impact of Pluronic® F68 on hollow fiber filter-based perfusion culture performance." Bioprocess and Biosystems Engineering 40 (2017): 1317-1326.

10. Tharmalingam, Tharmala, and Chetan T. Goudar. "Evaluating the impact of high Pluronic® F68 concentrations on antibody producing CHO cell lines." Biotechnology and Bioengineering 112.4 (2015): 832-837.

11. Sieblist, Christian, Marco Jenzsch, and Michael Pohlscheidt. "Influence of pluronic F68 on oxygen mass transfer." Biotechnology progress 29.5 (2013): 1278-1288.

12. Peng, Haofan, et al. "Mechanism investigation for poloxamer 188 raw material variation in cell culture." Biotechnology Progress 32.3 (2016): 767-775.

13. Šrom, Ondřej, et al. "Investigation of poloxamer cell protective ability via shear sensitive aggregates in stirred aerated bioreactor." Biochemical Engineering Journal 186 (2022): 108549.

14. Predictable Protection and Performance With Poloxamer 188 EMPROVE® EXPERT cell culture grades, Lit No. TB1249EN00.

15. Wilkinson, Peter M., Herman Haringa, and Laurent L. Van Dierendonck. "Mass transfer and bubble size in a bubble column under pressure." Chemical Engineering Science 49.9 (1994): 1417-1427.

16. Bouaifi, Mounir, et al. "A comparative study of gas hold-up, bubble size, interfacial area and mass transfer coefficients in stirred gas–liquid reactors and bubble columns." Chemical engineering and processing: Process intensification 40.2 (2001): 97-111.

17. Kapic, A., and Theodore J. Heindel. "Correlating gas-liquid mass transfer in a stirred-tank reactor." Chemical Engineering Research and Design 84.3 (2006): 239-245.

18. Garcia-Ochoa, Félix, and Emilio Gomez. "Theoretical prediction of gas–liquid mass transfer coefficient, specific area and hold-up in sparged stirred tanks." Chemical engineering science 59.12 (2004): 2489-2501.

19. McAndrew, Jake, and Greg Kauffman. "Characterizing the Effects of Antifoam C Emulsion on Oxygen Mass Transfer within the BIOne Drilled-Hole Sparger and Microsparger Single-Use Bioreactor Systems." Distek, White Paper No. 213 (2021)

20. Morao, A., et al. "Effect of antifoam addition on gas-liquid mass transfer in stirred fermenters." Bioprocess Engineering 20 (1999): 165-172.

Related Documents

1.Scalability and performance guide (PG12163EN)

2.BPI Sparger Poster (PS9879EN)

3.BPI 2022 Impeller Poster (PS9878EN)

4. A comparative analysis of mixing characterization methods in stirred tanks (WP11699EN)

5.Mobius® iFlex Bioreactor Datasheet (DS12340EN)

6.Mobius® 3L Bioreactor Specifications (SP2345000)

MilliporeSigma
400 Summit Drive Burlington, MA 01803

For additional information, please visit **SigmaAldrich.com**

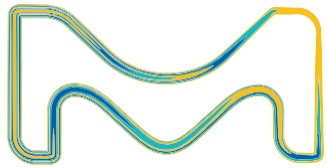

Lit. No. MS_WP12656EN
Ver. 0.1
02/2024